The Diagnostic And Prognostic Value of DYNLL1 And RAN In Lung Adenocarcinoma

Lei Cao
PUMCH: Peking Union Medical College Hospital
Hongsheng Liu
PUMCH: Peking Union Medical College Hospital
Zhili Cao
PUMCH: Peking Union Medical College Hospital
Naixin Liang
PUMCH: Peking Union Medical College Hospital
Chao Gao
PUMCH: Peking Union Medical College Hospital
Zhongxin Bing
PUMCH: Peking Union Medical College Hospital
Shanqing Li (lishanqing1966@outlook.com)
PUMCH: Peking Union Medical College Hospital https://orcid.org/0000-0001-5327-3772

Research Article

Keywords: Diagnostic, Prognostic, DYNLL1, RAN, Lung adenocarcinoma

Posted Date: August 4th, 2021

DOI: https://doi.org/10.21203/rs.3.rs-746416/v1

Abstract

Background: Lung adenocarcinoma (LUAD) is the most heterogeneous and aggressive among all NSCLC subtypes. This work aimed to determine the predictive ability of DYNLL1 and RAN in LUAD, as well as to explore the role of possible DYNLL1 and Ran molecular mechanisms on LUAD malignant behavior.

Methods: Using data from the Cancer Genome Atlas and the Genotype-Tissue Expression, we compared the expression of DYNLL1 and its related gene RAN in LUAD and normal lung tissues. We also studied the prognostic value of DYNLL1 and RAN in terms of overall survival (OS) in LUAD, liver cancer and renal cancer patients. Using data from the online database STRING, we further investigated the protein–protein interaction (PPI), miRNA and transcription factor regulatory networks of DYNLL1 and Ran. Then, molecular docking was used to obtain accurate combination models between molecular compounds and DYNLL1 or Ran. We also studied whether DYNLL1 and RAN influence the proliferation and migration of tumor cells with the stable knockdown LUAD cell lines.

Results: The expression of DYNLL1 and RAN was significantly upregulated in LUAD tissues compared to normal controls. And high expressions of DYNLL1 and RAN were associated with unfavorable overall survival in LUAD patients. We also found that knockdown of DYNLL1 and RAN inhibit the proliferation and migration of A549 tumor cells.

Conclusions: Overall, our study provides evidence that DYNLL1 and RAN are essential for the progression of LUAD. And they may serve as potential tumor biomarkers for the diagnosis and prognosis of patients with LUAD.

Introduction

As the most common type of non-small-cell lung cancer (NSCLC), lung adenocarcinoma (LUAD) accounts for more than 50% of NSCLC [1]. The morphological and molecular classification of LUAD has undergone substantial changes in recent years, resulting in a classification scheme more in tune with patient prognosis and survival. Earlier studies revealed that activation of the EGFR, KRAS, and ALK genes defines three different pathways that are responsible for a considerable fraction of LUAD [2]. Currently, some of the newer factors have found targetable drug molecules. Meanwhile, part of them have been included in current standard of clinical practice. This change in practice requires further development of detection methods [3]. Consequently, it is extremely important to identify molecular biomarkers that predict the diagnosis and prognosis of patients with LUAD, and potential new targets for molecular inhibition [4–6].

The LC8 family members of dynein light chain (DYNLL) were regarded as cargo adapters of molecular motors in some early studies [7–9]. And now, many studies have shown that they can act as hub proteins, interacting with short linear motifs located in intrinsically disordered protein fragments [10]. The LC8 family members of dynein light chain 1 (DYNLL1) is highly conserved among different species and widely expressed in many tissues [11]. It has been considered to be the main regulator of several cellular functions ranging from intracellular trafficking to apoptosis. For instance, the association of DYNLL1 and

neuronal nitric oxide synthase can inhibit the pro-apoptotic function [12]. DYNLL1 also interacts and interferes with BimL which belongs to the pro-apoptotic Bcl-2 family [13]. Previous studies have suggested that overexpression and phosphorylation of DYNLL1 promote the growth of breast cancer cells. DYNLL1 phosphorylation by p21-activated kinase 1 has been shown to promote the survival and growth of oestrogen receptor (ER)-positive breast cancer cells [14, 15]. On the other hand, the downregulation of DYNLL1 compromises the ER-nuclear accumulation and also its transactivation activity, suggesting that DYNLL1 has a potential chaperone-like activity in the nuclear translocation of ER. These data define an important role of DYNLL1–ER interaction in supporting and strengthening ER-induced cellular responses in breast cancer cells [16].

Ras-related nuclear protein (Ran) is a small GTPase and a member of the Ras superfamily. As a molecular switch that modulates the GTP/GDP cycle, Ran functions with a variety of Ran-binding proteins to control a wide range of fundamental cellular functions, including mitotic spindle assembly, nucleocytoplasmic transport, nuclear pore complex formation and nuclear envelope, which finally influence cell fate determination, including cell proliferation, differentiation, malignant transformation and cell death [17]. Overexpression of Ran GTPase has been observed in various cancer types, including colon, stomach, kidney, ovarian and pancreas cancer [18–20]. The upregulation of Ran expression may be a vital event in cell transformation and tumor progression [18]. Genetic instability is a well-known hallmark of cancer. Meanwhile, Ran GTPase plays a huge role in the mitotic instability of cancer cells [21]. Many studies have shown that the unusual localization of tumor suppressor proteins or oncogenes can be affected by Ran GTPase signaling in diverse types of cancer [22]. In detail, the localization of Ran-GTP is in the nucleus whereas Ran-GDP is restricted in the cytosol of cells. The GTP/GDP switch permits Ran to migrate across nuclear pore complexes and carry mRNA and protein along with it. Any instabilities in Ran expression has been shown to cause the abnormal transport of some tumor oncogenes such as NF-κB or Akt [23].

It has been reported that DYNLL1 is required for normal lung morphogenesis and ciliogenesis [24]. Meanwhile, RAN is associated with the occurrence and progression of many different types of cancer. However, the role of DYNLL1 in LUAD and its relationship to RAN has not yet been explicated. In this study, we found that the expression level of DYNLL1 and RAN was higher in LUAD tissues than normal lung tissues. And the high expression of DYNLL1 and RAN was correlated with poor overall survival in lung adenocarcinoma, liver cancer and renal cancer patients. Knockdown of DYNLL1 and RAN inhibit the proliferation and migration of A549 tumor cells. Collectively, DYNLL1 and RAN may be powerful biomarkers to support the diagnosis and prognosis of lung adenocarcinoma as well as potential tumor treatment targets.

Methods

Data mining.

GEPIA2 (http://gepia2.cancer-pku.cn) [25], Xena Browser (http://xena.ucsc.edu/) [26] and The Human Protein Atlas (https://www.proteinatlas.org/), three online interactive web server for analyzing the RNA sequencing data of tumors and normal samples from the TCGA and GTEx projects, were used to analyze the expression profiles and prognostic value of DYNLL1 and RAN. The clinicopathological information, including age at initial pathologic diagnosis, smoking history, gender, pathologic stage, recurrence status, relapse-free survival (RFS) in months, overall survival (OS) status, and OS in months was downloaded from the TCGA database.

Cell line

The A549 human lung adenocarcinoma cell line (RRID: CVCL_0023) was were obtained from the American Type Culture Collection and maintained in Dulbecco's modified Eagle's medium (DMEM) basic medium supplemented with 10% fetal bovine serum and 1% antibiotics at 37 °C with 5% CO_2.

Establishment of stable DYNLL1 and RAN knockdown cells

HEK-293T (RRID: CVCL_0063) cells were transfected with the packaging vector psPAX2, envelope plasmid pVSVG, and transfer plasmid containing the shRNA targeting DYNLL1 and RAN. A549 cells were treated with the lentivirus contain shRNAs and selected with puromycin (50 ng/μl). Sequences of used shRNAs were as follow: DYNLL1-shRNA-1: 5'-CCGGACAAGGACTGCAGCCTAAATTCTCGAGAATTTAGGCTGCAGTCCTTGTTTTTTG -3', DYNLL1-shRNA-2: 5'- CCGGTGGCCATTCTTCTGTTCAAATCTCGAGATTTGAACAGAAGAATGGCCATTTTTG -3', DYNLL1-shRNA-3: 5'- CCGGCCAAATACCAGAGACTGAAATCTCGAGATTTCAGTCTCTGGTATTTGGTTTTTG -3', DYNLL1-shRNA-4: 5'- CCGGGGGAGGAACTTCGGTAGTTATCTCGAGATAACTACCGAAGTTCCTCCCTTTTTG -3', DYNLL1-shRNA-5: 5'- CCGGACCAAACACTTCATCTACTTCCTCGAGGAAGTAGATGAAGTGTTTGGTTTTTTG -3', RAN-shRNA-1: 5'- CCGGACGTCATTTGACTGGTGAATTCTCGAGAATTCACCAGTCAAATGACGTTTTTTG -3', RAN-shRNA-2: 5'- CCGGGACCCTAACTTGGAATTTGTTCTCGAGAACAAATTCCAAGTTAGGGTCTTTTTG -3', RAN-shRNA-3: 5'- CCGGACGTCATTTGACTGGTGAATTCTCGAGAATTCACCAGTCAAATGACGTTTTTTG -3', RAN-shRNA-4: 5'- CCGGGACCCTAACTTGGAATTTGTTCTCGAGAACAAATTCCAAGTTAGGGTCTTTTTG -3', RAN-shRNA-5: 5'- CCGGGCACAGTATGAGCACGACTTACTCGAGTAAGTCGTGCTCATACTGTGCTTTTTG -3', scrambled-shRNA: 5'-CCGGGCGCGATAGCGCTCATAGTTTCTCGAGAATTAATTAACGCTATCGCGCTTTTTTG-3'.

Western blotting

Cellular DYNLL1 and RAN protein levels in A549 cells were evaluated in total cell extracts by Western blot analysis. Antibodies against RAN (RRID:AB_560865) was from Invitrogen (Carlsbad, CA, USA). Antibodies against DYNLL1 (RRID:AB_2093654) and β-actin (RRID:AB_306371) were from Abcam (Cambridge, UK). The protein bands were quantified relative to β-actin expression using ImageJ software (NIH, Bethesda, MD, USA, RRID:SCR_003070).

RNA extraction and qRT-PCR

Total RNAs were extracted with TRIzol reagent (Invitrogen, Carlsbad, CA, USA), reverse transcribed with PrimeScrip RT-PCR Kit (Takara Biotechnology Co., Ltd., Dalian, China), followed by qRT-PCR with SYBR Premix Ex Taq (Takara Biotechnology Co., Ltd., Dalian, China). The primers for DYNLL1were forward 5'- AGAGATGCAACAGGACTCGGT-3' and reverse 5'- CCAGGTGGGATTGTACTTCTTG-3'. The primers for RAN were forward 5'- GGTGGTACTGGAAAAACGACC -3' and reverse 5'- CCCAAGGTGGCTACATACTTCT -3'. The primers for ACTB (Beta-Actin) were forward 5'-CTGTCCCTGTATGCCTCTG-3' and reverse 5'-ATGTCACGCACGATTTCC-3'. ACTB was used as an internal control.

Cell proliferation analysis

Control and the DYNLL1 and RAN knockdown A549 cells (2×10^3 cells per well) were plated in 48-well plates and cultured for 72 h. Cell proliferation was determined using the colorimetric Cell Counting Kit-8 (CCK-8, Dojindo Laboratories, Kumamoto, Japan).

Cell migration analysis

A total of 5×10^5 cells were added in a volume of 100 μl (for flow conditions 340 μl) to the upper chamber of a 24-well transwell plate with a 8 μm pore in the insert (Corning International, Corning, NY). Lower wells contained 10% fetal bovine serum. The cells that migrated to the lower well after 6 hours were fixed and stained with crystal violet and counted with microscope. Each experiment was performed in triplicate at least three times.

Receiver operating characteristic (ROC) curve analysis.

The diagnostic value of the expression levels of DYNLL1, RAN, NKX2 and NAPSA in LUAD was studied by analyzing the expression data from 515 LUADs and 347 normal tissues. Specificity and sensitivity were plotted on the x- and y-axes, respectively. The area under curve (AUC) was calculated to assess the ability of the expression levels of DYNLL1, RAN, NKX2 and NAPSA to predict the outcome of patients with LUAD.

PPI network analysis and Functional enrichment

Protein–protein (PPI) interactions network can visualize the patterns of molecular interactions and help to explain the mechanisms underlying phenotypes. PPI network analysis was performed using the online database STRING (https://string-db.org/) [27]. And the Gene Ontology (GO) enrichment and Kyoto Encyclopedia of Genes and Genomes (KEGG) pathway analysis were analysed by STRING.

Construction of Target Genes-miRNA and Target Genes-TF Regulatory Network

The database DIANA-TarBase (http://diana.imis.athena-innovation.gr/DianaTools/index.php?r=tarbase/index) [28] was used to predicte the miRNAs which could target DYNLL1 and RAN. The network was created with Cytoscape software (http://www.cytoscape.org/, version 3.8.2, RRID:SCR_003032) [29].

The iRegulon (http://apps.cytoscape.org/apps/iRegulon) plugin[30] in Cytoscape was performed to predict and analyze the interaction pairs of target genes-transcription factor (TF) in the PPI network. The parameters were set as follows: 0.01 act as the minimum identity among orthologous genes, and 0.001 serve as the maximum false discovery rate on motif similarity. The higher score of Normalized Enrichment Score (NES) in output results represented the more reliable results. The TF-target interaction pairs whose NES > 4 were selected for the network construction.

The molecular docking for DYNLL1 and RAN

The Connectivity map database (https://www.broadinstitute.org/conne ctivity-map-cmap), designed by Broad Institute of MIT and Harvard, was used to search the small molecular compounds which have potential roles with DYNLL1 and RAN [31, 32]. To further understanding the docking mode of drug target, we obtained 3D structures of DYNLL1 and RAN from RCSB PDB (http://www.rcsb.org) and 3D structures of the small molecules which have potential roles with DYNLL1 and RAN from PubChem (https://pubchem.ncbi.nlm.nih.gov). Then we simulated a molecular docking using a web server Swissdock (http://www.swissdock.ch/docking), which was designed by Swiss Institute of Bioinformatics to predict the molecular interactions [33]. The 3D structures of DYNLL1 or RAN were uploaded as “Target selection” and those of small molecules as “Ligand selection” prior to a result report. Then, we used the USCF Chimera software (version 1.15, RRID:SCR_004097), a molecular modeling system, to calculate the possible binding modes and present an interactive visualization of data from Swissdock. The best docking simulation was ranked by the parameters of FullFitness and Estimated Energy.

Statistical Analysis

All statistical data were analyzed using SPSS 22.0 (SPSS, Chicago, IL, USA, RRID:SCR_002865) or GraphPad 7.0 (GraphPad Software, San Diego, CA, USA, RRID:SCR_002798). Chi square tests were used to analyze the associations between DYNLL1 and RAN expression levels and clinicopathological factors in the LUAD patients. Receiver operating characteristic (ROC) analysis were performed using SPSS 22.0 (Chicago, IL, USA). Diagnostic ability of the prediction model was evaluated, by calculating the area under a ROC curve. The ROC curve was drawn by plotting sensitivity against the false-positive rate. The cutoff value of DYNLL1 and RAN were calculated using the Youden index (specificity + sensitivity - 1). Kaplan–Meier curves of OS and RFS were generated using GraphPad 7.0 (GraphPad Software, San Diego, CA, USA). Data were presented as mean ±SD. P values < 0.05 were considered statistically significant.

Results

The correlation between the expression of DYNLL1 and RAN in LUAD

In order to find potential tumor biomarkers for the diagnosis and prognosis of patients with LUAD as well as new factors involved in the development of LUAD, we analysis the top factors which influence the relapse-free survival and overall survival in LUAD through the GEPIA2 database. And we found that DYNLL1 was among the top factors which significant influence the overall survival time in LUAD.

Meanwhile, there were few researches focused on the role of DYNLL1 in cancer development, especially in lung cancer. Furthermore, the expression of DYNLL1 was significantly upregulated in LUAD samples than adjacent normal tissues (Fig. 1A). Further analysis showed that the expression level of RAN had positive correlation ($r^2 = 0.248$, $P < 0.0001$) with DYNLL1 (Fig. 1B). LUAD patients with higher expression levels of DYNLL1 always had higher expression levels of RAN. Meanwhile, the expression of RAN was also upregulated in LUAD samples (Fig. 1C). Heatmap also showed that DYNLL1 and RAN expression was significantly higher in LUAD tissues than in normal tissues (Fig. 1D).

Diagnostic value of DYNLL1 and RAN for LUAD patients

Since the expression levels of DYNLL1 and RAN were upregulated in LUAD samples compared with controls, we next explored whether DYNLL1 and RAN may serve as potential diagnostic biomarkers in LUAD. ROC curve analysis was used to investigate the diagnostic value of DYNLL1 and RAN in distinguishing LUAD patients from normal conditions. The results showed that the AUC of DYNLL1 was 0.818 and the optimal cut-off value was 11.95, with a sensitivity of 76.5% and specificity of 71.1% ($P < 0.0001$) (Fig. 2A). For RAN, the AUC was 0.994 and the cut-off value was 12.82, with a sensitivity and specificity of 95.3% and 92.9%, respectively ($P < 0.0001$) (Fig. 2B). As positive controls, we also analysed the ROC curves of two well-known diagnosis biomarkers, thyroid transcription factor 1 (TTF-1/NKX2-1) and napsin-A (NAPSA), in LUADs. The results indicated that the performance of the NKX2-1 [AUC, 0.570; 95% CI (confidence interval), 0.528–0.612] (Fig. 2C) and NAPSA (AUC, 0.515; 95% CI, 0.473–0.557) (Fig. 2D) were not satisfactory than DYNLL1 or RAN, which showed lower sensitivity and specificity than DYNLL1 and RAN. These results indicate that DYNLL1 and RAN have huge potential diagnose value for LUAD.

High DYNLL1 and RAN expressions were independent prognostic factors for poor OS and RFS in LUAD

The associations between DYNLL1 and RAN expression and the demographic and clinicopathological parameters in patients with LUAD were summarized in Table 1. The results showed that the high DYNLL1 expression group had significantly higher mutation numbers (42/101, 41.6% *vs.* 35/129, 27.1%, $P = 0.013$) than the low DYNLL1 expression group. In addition, the high RAN expression group had a significantly higher proportions of male (103/196, 52.6% vs. 137/321, 42.7%, $P = 0.035$) and advanced neoplasm disease stage (53/193, 27.5% vs. 57/316, 18.0%, $P = 0.011$) compared with the low RAN expression group. In LUAD, the expression of DYNLL1 showed no differences among different pathological stages (Fig. 2E). Strikingly, RAN expression gradually enhanced with the increase of pathological stages (Fig. 2F). By conducting multivariate analysis, we found that, in addition to clinical stage, the expression levels of DYNLL1 and RAN were all independent prognostic factor for poor OS (HR = 0.694 and $P = 0.014$ for DYNLL1; HR = 0.575 and $P < 0.001$ for RAN) and RFS (HR = 0.543 and $P = 0.002$ for DYNLL1; HR = 0.521 and $P = 0.001$ for RAN) in LUAD patients (Table 2).

Table 1: Statistically significant associations of neoplasm disease stage, DYNLL1 and RAN mRNA expression with relapse-free survival (RFS), overall survival (OS) in LUAD patients, assessed in multivariate Cox proportional hazard models.

Outcome	RFS			OS		
	HR	95% CI	*P* value	HR	95% CI	*P* value
Neoplasm Disease Stage (I, II *vs*. III, IV, V)	0.583	0.409-0.832	0.003	0.376	0.276-0.512	<0.001
DYNLL1 expression level (high *vs*. low)	0.543	0.370-0.797	0.002	0.694	0.519-0.928	0.014
RAN expression level (high *vs*. low)	0.521	0.356-0763	0.001	0.575	0.430-0.770	<0.001
DYNLL1 & RAN co-expression level (high *vs*. low)	0.422	0.269-0.660	<0.001	0.533	0.381-0.746	<0.001

Table 2: Association of DYNLL1 and RAN expression levels with clinicopathologic variables of LUAD patients.

Outcome	DYNLL1 expression			RAN expression		
	Low	High	*P* value	Low	High	*P* value
Age / year (n=490) †			0.851			0.099
65	119	98		134	87	
≥65	161	112		179	98	
Gender (n=517)			0.160			0.035
Male	128	112		137	103	
Female	168	109		184	93	
Mutations / number (n=230)			0.013			0.316
≤230	94	59		100	53	
230	35	42		42	35	
Smoking history / Category‡ (n=503)			0.067			0.475
1	47	29		54	22	
2, 3, 4, 5	243	184		259	168	
Neoplasm Disease Stage (n=509)	221	163	0.741	259	140	0.011
I, II						
III, IV, V	59	47		57	53	

† n: Number

‡ Smoking history: 1: lifelong non-smoker; 2: current smoker; 3. Current reformed smoker (for>15 years); 4. Current reformed smoker (for≤15 years); 5. Current reformed smoker (duration not specified).

High DYNLL1 and RAN expression was associated with unfavorable outcomes in LUAD patients

In order to reveal association between DYNLL1 and RAN gene expression levels and LUAD prognosis, we extracted the survival data in TCGA database. Next, we performed Kaplan–Meier survival curves and the cancer patients were divided into high/low expression group by using the best cutoff model. The results showed that patients with lower expression levels of DYNLL1 and RAN have better overall survival prognoses than those with higher expression levels of these two genes in LUAD (P = 0.0028, Hazard Ratio = 0.629 and P = 0.0005, Hazard Ratio = 0.600, respectively) (Fig. 3A and Fig. 3B). Higher expression level of DYNLL1 also significantly associated with shorter relapse-free survival time (P = 0.0070, Hazard Ratio = 0.675) (Fig. 3C). Furthermore, the patients with both high expression of DYNLL1 and RAN showed the worst overall survival time (P < 0.0001, Hazard Ratio = 0.486) (Fig. 3D).

High DYNLL1 and RAN expression was associated with unfavorable outcomes in liver and renal cancer patients

We also investigated whether DYNLL1 and RAN expression could influence the patients' overall survival time in other 17 kinds of cancer types, including glioma, thyroid cancer, colorectal cancer, breast cancer and so on. Notably, results showed that the high expression of DYNLL1 and RAN had significantly worse OS compared to the low expression groups both in liver and renal cancer patients, respectively ($P < 0.0001$ for all, Hazard Ratio = 0.497, 0.506, 0.414, 0.506, respectively) (Fig. 4A, 4B, 4C and 4D). These results indicate that DYNLL1 and RAN participate in cancer development in a variety of cancer types.

Protein-protein interaction network analysis

In order to study how DYNLL1 and RAN were involved in the development of LUAD, STRING was performed to construct the protein-protein interactions between DYNLL1 and RAN. In the PPI network, DYNLL1 and RAN had close connections through RANBP1/2, RANGAP1, NUTF2 and XPO1/5 (Fig. 5). Furthermore, we did functional analysis based on the PPI network. The top processes and pathways were showed in Table 3. The analysis revealed that DYNLL1 and RAN may interact through intracellular protein transport pathways and participate the microtubule-based process and mitotic cell cycle process.

Table 3 Functional and pathway enrichment analysis.

Category	ID	Term Description	Observed gene count	Background gene count	P-value
Biological process (go)	GO:0006886	intracellular protein transport	10	836	1.85E-10
	GO:0034613	cellular protein localization	11	1367	2.56E-10
	GO:0016032	viral process	8	571	6.32E-09
	GO:0031503	protein-containing complex localization	6	223	3.47E-08
	GO:0007017	microtubule-based process	7	605	2.75E-07
	GO:1903047	mitotic cell cycle process	6	564	6.34E-06
	GO:0051640	organelle localization	5	574	0.00012
	GO:0006996	organelle organization	8	3131	0.00075
	GO:0044093	positive regulation of molecular function	6	1713	0.0015
	GO:0044085	cellular component biogenesis	7	2556	0.0016
Enrichment. Function	GO:0008536	Ran GTPase binding	8	35	1.45E-17
	GO:0019899	enzyme binding	9	2197	8.38E-06
	GO:0005515	protein binding	12	6605	3.33E-05
	GO:0046982	protein heterodimerization activity	4	519	0.0015
Enrichment. Component	GO:0032991	protein-containing complex	11	4792	2.47E-05
	GO:0005829	cytosol	11	4958	3.01E-05
	GO:0043232	intracellular non-membrane-bounded organelle	10	4005	5.42E-05

	GO:0012505	endomembrane system	10	4347	9.45E-05
	GO:0015630	microtubule cytoskeleton	6	1118	0.00016
	GO:0005815	microtubule organizing center	5	683	0.00021
	GO:0044446	intracellular organelle part	12	8882	0.00043
	GO:0005634	nucleus	11	6892	0.00044
	GO:0044430	cytoskeletal part	6	1547	0.00071
	GO:0005737	cytoplasm	12	11238	0.0045
Enrichment. KEGG	hsa03013	RNA transport	7	159	1.48E-11
	hsa04962	Vasopressin-regulated water reabsorption	2	44	0.0012
	hsa05166	HTLV-I infection	3	250	0.0012
	hsa03008	Ribosome biogenesis in eukaryotes	2	76	0.0018
	hsa05169	Epstein-Barr virus infection	2	194	0.0086
Enrichment. Keyword	KW-0813	Transport	9	1973	4.82E-06
	KW-0007	Acetylation	10	3335	1.31E-05
	KW-0945	Host-virus interaction	5	432	3.99E-05
	KW-0539	Nucleus	10	5200	0.00045
	KW-1017	Isopeptide bond	6	1713	0.0014
	KW-0963	Cytoplasm	9	4972	0.0022
	KW-0832	Ubl conjugation	6	2380	0.0069
	KW-0597	Phosphoprotein	10	8066	0.0139

Construction of target genes-TF and target genes-miRNA regulatory network

Furthermore, we constructed the Target Genes-Transcription factors (TFs) Regulatory Network. As shown in Fig. 6A, there were 16 TFs (E2F1, TP53, ZNF143, and so on) had been predicted to regulate both DYNLL1 and RAN. And there had other 29 TFs and 6 TFs been predicted to regulate DYNLL1 (ex, SMAD4, ELF1) and RAN (ex, MYC, CEBPB), respectively.

MicroRNAs (miRNAs) play critical roles in tumor progression. So, we analysed the miRNAs which have potential roles to regulate the expression of DYNLL1 and RAN. As shown in Fig. 6B-6C, DYNLL1 interacts with 10 miRNAs (hsa-miR-92a-3p, for example), RAN interacts with 97 miRNAs (has-miR-197-3p, for example).

Identification of candidate drugs target to DYNLL1 and RAN

The next question was to identify candidate drugs that were available to target DYNLL1 and RAN. Based on Connectivity map database, we screened the small molecular compounds which have potential roles with DYNLL1 and RAN. We found that ampiroxicam, 5-iodotubercidin, and pidorubicine had the highest possibility to interact with DYNLL1. And SCH-79797, GBR-12935, and ouabain had the highest possibility to interact with RAN. Then, the compounds were used to construct the molecular docking model with DYNLL1 and RAN, respectively. The Swissdock was used to generated a series of docking modes and USCF Chimera software was used to present an interactive visualization of data from Swissdock. The docking mode of the complex were shown in Fig. 7.

Knockdown of DYNLL1 and RAN inhibit the proliferation and migration of A549 tumor cells

To further understand the role of DYNLL1 and RAN in the development of LUAD, we generated stable DYNLL1 and RAN knockdown cells by transfection with DYNLL1 and RAN -specific short hairpin RNAs (shRNAs), respectively. The knockdown efficiency of DYNLL1 in A549 cells were confirmed by both qRT-PCR and Western blotting (Fig. 8A-8B). And DYNLL1-shRNA-1 and DYNLL1-shRNA-5 showed higher knockdown efficiency (Fig. 8A-8B). Moreover, we investigated the effect of DYNLL1 knockdown on A549 cell proliferation. The results showed that knockdown of DYNLL1 significantly inhibited the proliferation of A549 tumor cells (Fig. 8C). Meanwhile, the knockdown efficiency of RAN in A549 cells were showed in Fig. 8D-8E and RAN-shRNA-3 and RAN-shRNA-5 showed higher knockdown efficiency. Furthermore, the knockdown of RAN also restrained the proliferation of A549 tumor cells (Fig. 8F). We next explored whether DYNLL1 and RAN influence the migration of A549 tumor cells. And the results showed that both knockdown of DYNLL1 and RAN in A549 cells suppressed the migration ability of tumor cells (Fig. 8G-8H). These results indicated that DYNLL1 and RAN may promote the proliferation and migration of tumor cells in the development of LUAD.

Discussion

In this study, we identified the aberrantly expressed DYNLL1 and RAN involved in LUAD through the comparison of RNA expression profiles in cancerous tissues with that of normal lung tissues based on validation from TCGA and GTEx datasets. Additionally, we discovered that the expression of DYNLL1 and

RAN significantly predicted the overall survival time in patients with LUAD. And knockdown of DYNLL1 and RAN inhibit the proliferation and migration of A549 tumor cells.

Previous studies have suggested that DYNLL1 is a physiologic substrate of p21-activated kinase 1 (Pak1). And the DYNLL1-Pak1 interaction plays a critical role in breast cancer cell survival [14]. Additionally, as an inhibitor of DNA end resection, DYNLL1 also significantly influences genomic stability and response to chemotherapy-induced DNA damaging. The loss of DYNLL1, induced DNA end resection and restored homologous recombination (HR), was shown to contributed to the cisplatin and olaparib resistance in BRCA1-deficient high-grade serous ovarian carcinoma (HGSOC) cells [34]. Another study showed that DYNLL1 could act as a protein hub for the 53BP1 oligomerisation and its recruitment to DSBs [35]. These studies led us to highlighting a novel role of DYNLL1 in cancer progression rather than a motor that transports cargo along microtubules.

Ran GTPase plays important roles in cell cycle progression through the regulation of the microtubule polymerization, mitotic spindle formation, and cytoskeleton organization during mitosis. Consequently, dysregulation of Ran could therefore lead to the microtubule dysfunction, aneuploidy and disruption in cell migration [36, 37]. Some study has shown that high expression of Ran GTPase promotes the invasion and metastasis in human clear cell renal cell carcinoma [38]. Moreover, Ran stimulates membrane targeting and stabilization of RhoA which enhances ovarian cancer cell invasion [39]. It is also found that the overexpression of Ran is correlated with metastasis potential in pancreatic cancers. Additionally, the knockdown of RAN significantly inhibited the capability of pancreatic cancer cells to metastasize to the liver [40]. Consistently, overexpression of RAN leads to the activation of PI3K/AKT signaling and promotes invasive ability in non-small cell lung cancer cells [41]. Strikingly, Ran expression is essential for mitosis of cancer cells but not normal cells [19, 42]. It has been shown that Ran expression is more important to tumor cells with K-Ras activating mutations than the K-Ras wild-type normal cells [43]. In another study, cancer cells with hyperactivation of the Ras/MEK/ERK and PI3K/Akt/mTORC1 pathways are more dependent on Ran expression than their wild-type counterparts [44]. On the other hand, Ran GTPase has also been implicated in drug resistance and cancer therapeutic development. The inactivation of Ran GTPase can significantly increase the sensitivity of breast cancer cells to gefitinib [45]. Furthermore, functional depletion of Ran GTPase suppresses the proliferation and migration of both glioblastoma and breast cancer cells [46]. It was also showed that the inhibition of Ran in SCID mice can induced ovarian cancer regression [47].

In our study, we found that DYNLL1 and RAN were co-expressed in LUAD patients. And high expression of DYNLL1 and RAN associated with unfavorable overall survival in LUAD patients. Notably, DYNLL1 was most well-regarded as cargo adapters of molecular motors. Meanwhile, Ran GTPase could also function as transporter. The co-expression of the two proteins may strengthen the transportation and hyperactivation of oncogenes. Combined the protein-protein interaction and functional enrichment analysis, the top pathways that DYNLL1 and Ran participate in including intracellular protein transport, cellular protein localization, microtubule-based process and mitotic cell cycle process. We proposed that

DYNLL1 and Ran may promote the LUAD development through the influence of oncoprotein transportation or directly regulates cell mitosis.

In target genes-miRNA regulatory networks, RAN interacts with more miRNAs than DYNLL1. On the other hand, in target genes-TF regulatory network, DYNLL1 seems to be regulated by more transcription factors that of RAN. We also investigated the candidate drugs which could target DYNLL1 and RAN. Ampiroxicam is a prodrug of piroxicam which is an anti-inflammatory agent [48]. Pidorubicine, also known as epirubicin, is a 4'-epi-isomer of doxorubicin. And pidorubicine has shown good antitumor effects by interference with the synthesis and function of DNA [49]. The two drugs could be good candidates to interact with DYNLL1 in the treatment of LUAD. Ouabain is a cardiotonic steroid hormone which has a role as some ATPase inhibitor. Whether it could be a candidate to interact with Ran in the treatment of LUAD need more studies. The detailed mechanisms of DYNLL1 and Ran involved in LUAD development are intriguing questions needed to be investigated.

Conclusions

Altogether, the results presented here indicate that DYNLL1 and RAN play important roles in the development of lung adenocarcinoma, and their expression could serve as independent factors to predict the poor prognosis of LUAD patients. Knockdown of DYNLL1 and RAN impair the proliferation and migration of A549 tumor cells. DYNLL1 and RAN may become powerful biomarkers to support the diagnosis and prognosis of lung adenocarcinoma as well as potential treatment targets.

Declarations

Ethics approval and consent to participate

Not applicable. There were no tissue or animal studies, and all clinical data comes from database open to the public.

Consent for publication

Not applicable. There were no individual person’s data in the study.

Acknowledgements

Not applicable.

Funding

This study was supported by Chinese Academy of Medical Sciences Innovation Fund for Medical Sciences (2017-I2M-1-009).

Availability of data and materials

The datasets used and/or analyzed during the present study are available from the corresponding author on reasonable request.

Authors' contributions

(I) Conception and design: L Cao, H Liu and S Li;

(II) Administrative support: S Li

(III) Provision of study materials: L Cao and S Li

(IV) Collection and assembly of data: L Cao, H Liu, Z Cao, N Liang, C Gao and Z Bing

(V) Data analysis and interpretation: L Cao, H Liu and S Li

(VI) Manuscript writing: All authors

(VII) Final approval of manuscript: All authors

Footnote

Conflicts of Interest: The authors have no conflicts of interest to declare.

Ethical statement: The authors are accountable for all aspects of the work in ensuring that questions related to the accuracy or integrity of any part of the work are appropriately investigated and resolved.

References

1. Siegel RL, Miller KD, Jemal A: **Cancer statistics, 2019.** *CA Cancer J Clin* 2019, **69:**7-34.

2. Janku F, Stewart DJ, Kurzrock R: **Targeted therapy in non-small-cell lung cancer--is it becoming a reality?** *Nat Rev Clin Oncol* 2010, **7:**401-414.

3. Chen X, Lu J, Wu Y, Jiang X, Gu Y, Li Y, Zhao H, Jin M: **Genetic features and application value of next generation sequencing in the diagnosis of synchronous multifocal lung adenocarcinoma.** *Oncol Lett* 2020, **20:**2829-2839.

4. Rochigneux P, Garon EB: **Are lung adenocarcinoma mutations shaping the immune microenvironment?** *Transl Cancer Res* 2018, **7:**S740-S742.

5. Wang Y, Zhang L, Chen Y, Li M, Ha M, Li S: **Screening and identification of biomarkers associated with the diagnosis and prognosis of lung adenocarcinoma.** *J Clin Lab Anal* 2020**:**e23450.

6. Ye J, Liu H, Xu ZL, Zheng L, Liu RY: **Identification of a multidimensional transcriptome prognostic signature for lung adenocarcinoma.** *J Clin Lab Anal* 2019, **33:**e22990.

7. Pfister KK, Shah PR, Hummerich H, Russ A, Cotton J, Annuar AA, King SM, Fisher EM: **Genetic analysis of the cytoplasmic dynein subunit families.** *PLoS Genet* 2006, **2:**e1.

8. Wickstead B, Gull K: **Dyneins across eukaryotes: a comparative genomic analysis.** *Traffic* 2007, **8:**1708-1721.

9. Sakakibara H, Oiwa K: **Molecular organization and force-generating mechanism of dynein.** *FEBS J* 2011, **278:**2964-2979.

10. Rapali P, Szenes A, Radnai L, Bakos A, Pal G, Nyitray L: **DYNLL/LC8: a light chain subunit of the dynein motor complex and beyond.** *FEBS J* 2011, **278:**2980-2996.

11. Yang Z, Vadlamudi RK, Kumar R: **Dynein light chain 1 phosphorylation controls macropinocytosis.** *J Biol Chem* 2005, **280:**654-659.

12. Jaffrey SR, Snyder SH: **PIN: an associated protein inhibitor of neuronal nitric oxide synthase.** *Science* 1996, **274:**774-777.

13. Puthalakath H, Huang DC, O'Reilly LA, King SM, Strasser A: **The proapoptotic activity of the Bcl-2 family member Bim is regulated by interaction with the dynein motor complex.** *Mol Cell* 1999, **3:**287-296.

14. Vadlamudi RK, Bagheri-Yarmand R, Yang Z, Balasenthil S, Nguyen D, Sahin AA, den Hollander P, Kumar R: **Dynein light chain 1, a p21-activated kinase 1-interacting substrate, promotes cancerous phenotypes.** *Cancer Cell* 2004, **5:**575-585.

15. Mazumdar A, Kumar R: **Estrogen regulation of Pak1 and FKHR pathways in breast cancer cells.** *FEBS Lett* 2003, **535:**6-10.

16. Rayala SK, Den Hollander P, Balasenthil S, Yang Z, Broaddus R, Kumar R: **Functional regulation of oestrogen receptor pathway by the dynein light chain 1.** *EMBO Reports* 2005, **6:**538-544.

17. Nagai M, Yoneda Y: **Small GTPase Ran and Ran-binding proteins.** *Biomol Concepts* 2012, **3:**307-318.

18. Azuma K, Sasada T, Takedatsu H, Shomura H, Koga M, Maeda Y, Yao A, Hirai T, Takabayashi A, Shichijo S, Itoh K: **Ran, a small GTPase gene, encodes cytotoxic T lymphocyte (CTL) epitopes capable of inducing HLA-A33-restricted and tumor-reactive CTLs in cancer patients.** *Clin Cancer Res* 2004, **10:**6695-6702.

19. Xia F, Lee CW, Altieri DC: **Tumor cell dependence on Ran-GTP-directed mitosis.** *Cancer Res* 2008, **68:**1826-1833.

20. Abe H, Kamai T, Shirataki H, Oyama T, Arai K, Yoshida K: **High expression of Ran GTPase is associated with local invasion and metastasis of human clear cell renal cell carcinoma.** *International Journal of Cancer* 2008, **122:**2391-2397.

21. Saxena S, Gandhi A, Lim PW, Relles D, Sarosiek K, Kang C, Chipitsyna G, Sendecki J, Yeo CJ, Arafat HA: **RAN GTPase and Osteopontin in Pancreatic Cancer.** *Pancreat Disord Ther* 2013, **3:**113.

22. Kau TR, Way JC, Silver PA: **Nuclear transport and cancer: from mechanism to intervention.** *Nat Rev Cancer* 2004, **4:**106-117.

23. Abe H, Kamai T, Shirataki H, Oyama T, Arai K, Yoshida K: **High expression of Ran GTPase is associated with local invasion and metastasis of human clear cell renal cell carcinoma.** *Int J Cancer* 2008, **122:**2391-2397.

24. Goggolidou P, Stevens J, Agueci F, Keynton J, Wheway G, Grimes DT, Patel SH, Hilton H, Morthorst SK, Dipaolo A: **ATMIN is a transcriptional regulator of both lung morphogenesis and ciliogenesis.** *Development* 2014, **141:**3966-3977.

25. Tang Z, Kang B, Li C, Chen T, Zhang Z: **GEPIA2: an enhanced web server for large-scale expression profiling and interactive analysis.** *Nucleic Acids Res* 2019, **47:**W556-W560.

26. Cline MS, Craft B, Swatloski T, Goldman M, Ma S, Haussler D, Zhu JC: **Exploring TCGA Pan-Cancer Data at the UCSC Cancer Genomics Browser.** *Scientific Reports* 2013, **3**.

27. Szklarczyk D, Franceschini A, Wyder S, Forslund K, Heller D, Huerta-Cepas J, Simonovic M, Roth A, Santos A, Tsafou KP, et al: **STRING v10: protein-protein interaction networks, integrated over the tree of life.** *Nucleic Acids Research* 2015, **43:**D447-D452.

28. Vlachos IS, Paraskevopoulou MD, Karagkouni D, Georgakilas G, Vergoulis T, Kanellos I, Anastasopoulos IL, Maniou S, Karathanou K, Kalfakakou D, et al: **DIANA-TarBase v7.0: indexing more than half a million experimentally supported miRNA:mRNA interactions.** *Nucleic Acids Res* 2015, **43:**D153-159.

29. Shannon P, Markiel A, Ozier O, Baliga NS, Wang JT, Ramage D, Amin N, Schwikowski B, Ideker T: **Cytoscape: a software environment for integrated models of biomolecular interaction networks.** *Genome Res* 2003, **13:**2498-2504.

30. Janky R, Verfaillie A, Imrichova H, Van de Sande B, Standaert L, Christiaens V, Hulselmans G, Herten K, Naval Sanchez M, Potier D, et al: **iRegulon: from a gene list to a gene regulatory network using large motif and track collections.** *PLoS Comput Biol* 2014, **10:**e1003731.

31. Subramanian A, Narayan R, Corsello SM, Peck DD, Natoli TE, Lu X, Gould J, Davis JF, Tubelli AA, Asiedu JK, et al: **A Next Generation Connectivity Map: L1000 Platform and the First 1,000,000 Profiles.** *Cell* 2017, **171:**1437-1452 e1417.

32. Lamb J, Crawford ED, Peck D, Modell JW, Blat IC, Wrobel MJ, Lerner J, Brunet JP, Subramanian A, Ross KN, et al: **The Connectivity Map: using gene-expression signatures to connect small molecules, genes, and disease.** *Science* 2006, **313:**1929-1935.

33. Grosdidier A, Zoete V, Michielin O: **SwissDock, a protein-small molecule docking web service based on EADock DSS.** *Nucleic Acids Res* 2011, **39:**W270-277.

34. He YJ, Meghani K, Caron MC, Yang C, Ronato DA, Bian J, Sharma A, Moore J, Niraj J, Detappe A, et al: **DYNLL1 binds to MRE11 to limit DNA end resection in BRCA1-deficient cells.** *Nature* 2018, **563:**522-526.

35. Becker JR, Cuella-Martin R, Barazas M, Liu R, Oliveira C, Oliver AW, Bilham K, Holt AB, Blackford AN, Heierhorst J, et al: **The ASCIZ-DYNLL1 axis promotes 53BP1-dependent non-homologous end joining and PARP inhibitor sensitivity.** *Nat Commun* 2018, **9:**5406.

36. Dallol A, Hesson LB, Matallanas D, Cooper WN, O'Neill E, Maher ER, Kolch W, Latif F: **RAN GTPase is a RASSF1A effector involved in controlling microtubule organization.** *Curr Biol* 2009, **19:**1227-1232.

37. Jeon H, Zheng LT, Lee S, Lee WH, Park N, Park JY, Heo WD, Lee MS, Suk K: **Comparative analysis of the role of small G proteins in cell migration and cell death: cytoprotective and promigratory effects of RalA.** *Exp Cell Res* 2011, **317:**2007-2018.

38. Kurisetty VV, Johnston PG, Johnston N, Erwin P, Crowe P, Fernig DG, Campbell FC, Anderson IP, Rudland PS, El-Tanani MK: **RAN GTPase is an effector of the invasive/metastatic phenotype induced by osteopontin.** *Oncogene* 2008, **27:**7139-7149.

39. Zaoui K, Boudhraa Z, Khalife P, Carmona E, Provencher D, Mes-Masson AM: **Ran promotes membrane targeting and stabilization of RhoA to orchestrate ovarian cancer cell invasion.** *Nat Commun* 2019, **10:**2666.

40. Deng L, Shang Y, Guo S, Liu C, Zhou L, Sun Y, Nie Y, Fan D, Lu Y, Guo X: **Ran GTPase protein promotes metastasis and invasion in pancreatic cancer by deregulating the expression of AR and CXCR4.** *Cancer Biol Ther* 2014, **15:**1087-1093.

41. Ning J, Liu W, Zhang J, Lang Y, Xu S: **Ran GTPase induces EMT and enhances invasion in non-small cell lung cancer cells through activation of PI3K-AKT pathway.** *Oncology Research* 2014, **21:**67-72.

42. Simula MP, Marin MD, Caggiari L, De Re V, Cannizzaro R, Canzonieri V: **Comment re: Ran-GTP control of tumor cell mitosis.** *Cancer Res* 2009, **69:**1240; author reply 1240.

43. Morgan-Lappe SE, Tucker LA, Huang X, Zhang Q, Sarthy AV, Zakula D, Vernetti L, Schurdak M, Wang J, Fesik SW: **Identification of Ras-related nuclear protein, targeting protein for xenopus kinesin-like protein 2, and stearoyl-CoA desaturase 1 as promising cancer targets from an RNAi-based screen.** *Cancer Res* 2007, **67:**4390-4398.

44. Yuen HF, Chan KK, Grills C, Murray JT, Platt-Higgins A, Eldin OS, O'Byrne K, Janne P, Fennell DA, Johnston PG, et al: **Ran is a potential therapeutic target for cancer cells with molecular changes associated with activation of the PI3K/Akt/mTORC1 and Ras/MEK/ERK pathways.** *Clin Cancer Res* 2012, **18:**380-391.

45. Yuen HF, Chan KK, Platt-Higgins A, Dakir el H, Matchett KB, Haggag YA, Jithesh PV, Habib T, Faheem A, Dean FA, et al: **Ran GTPase promotes cancer progression via Met recepto-rmediated downstream signaling.** *Oncotarget* 2016, **7:**75854-75864.

46. Sheng KL, Pridham KJ, Sheng Z, Lamouille S, Varghese RT: **Functional Blockade of Small GTPase RAN Inhibits Glioblastoma Cell Viability.** *Front Oncol* 2018, **8:**662.

47. Barres V, Ouellet V, Lafontaine J, Tonin PN, Provencher DM, Mes-Masson AM: **An essential role for Ran GTPase in epithelial ovarian cancer cell survival.** *Mol Cancer* 2010, **9:**272.

48. Carty TJ, Marfat A, Moore PF, Falkner FC, Twomey TM, Weissman A: **Ampiroxicam, an anti-inflammatory agent which is a prodrug of piroxicam.** *Agents Actions* 1993, **39:**157-165.

49. Cersosimo RJ, Hong WK: **Epirubicin: a review of the pharmacology, clinical activity, and adverse effects of an adriamycin analogue.** *J Clin Oncol* 1986, **4:**425-439.

Figures

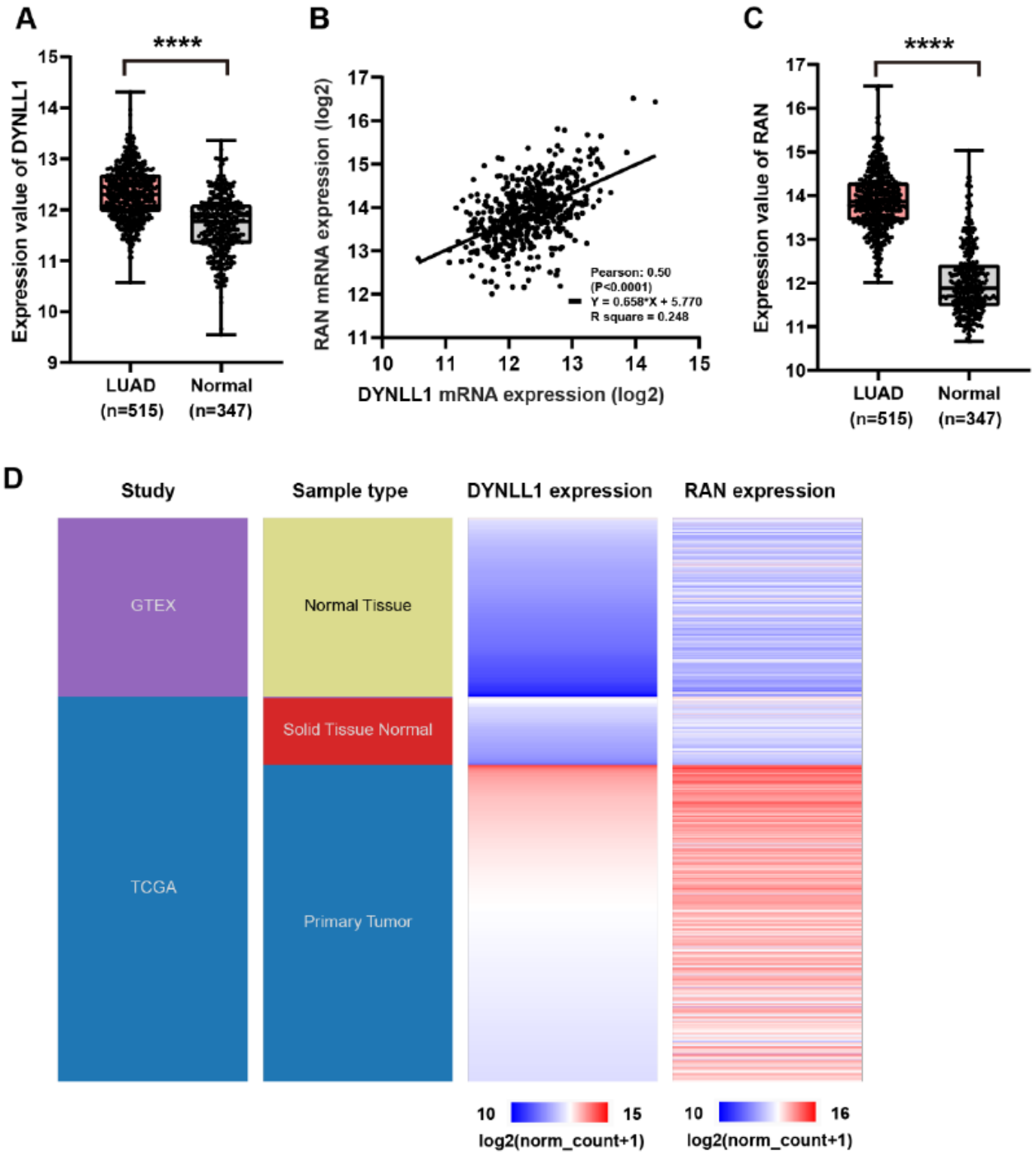

Figure 1

The expression levels of DYNLL1 and RAN were significantly upregulated in lung adenocarcinoma (LUAD). (A) Expression of DYNLL1 in LUAD and normal lung tissues. (B) Regression analysis of the correlation between DYNLL1 expression and RAN. (C) Expression of RAN in LUAD and normal lung tissues. (D) Heatmap of DYNLL1 and RAN expression in LUAD patients and normal lung tissues. ****, P<0.0001.

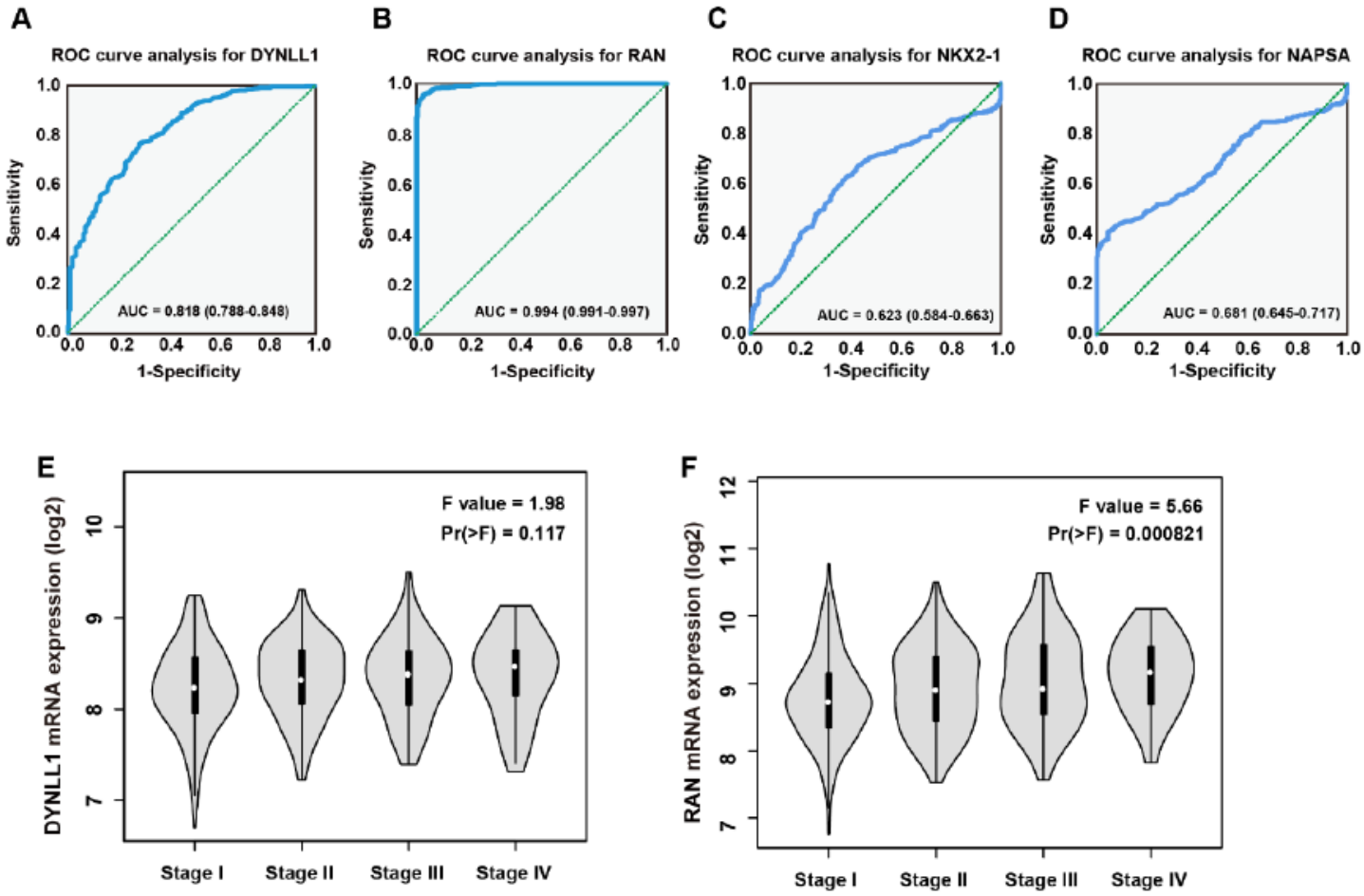

Figure 2

The diagnostic value of DYNLL1 and RAN expression in LUAD was evaluated using ROC curves. (A-D) Receiver operating characteristic curves for estimating the diagnostic value of DYNLL1(A), RAN(B), NKX2(C) and NAPSA(D), respectively. (E) DYNLL1 expression in different pathological stages of LUAD. (F) RAN expression in different pathological stages of LUAD.

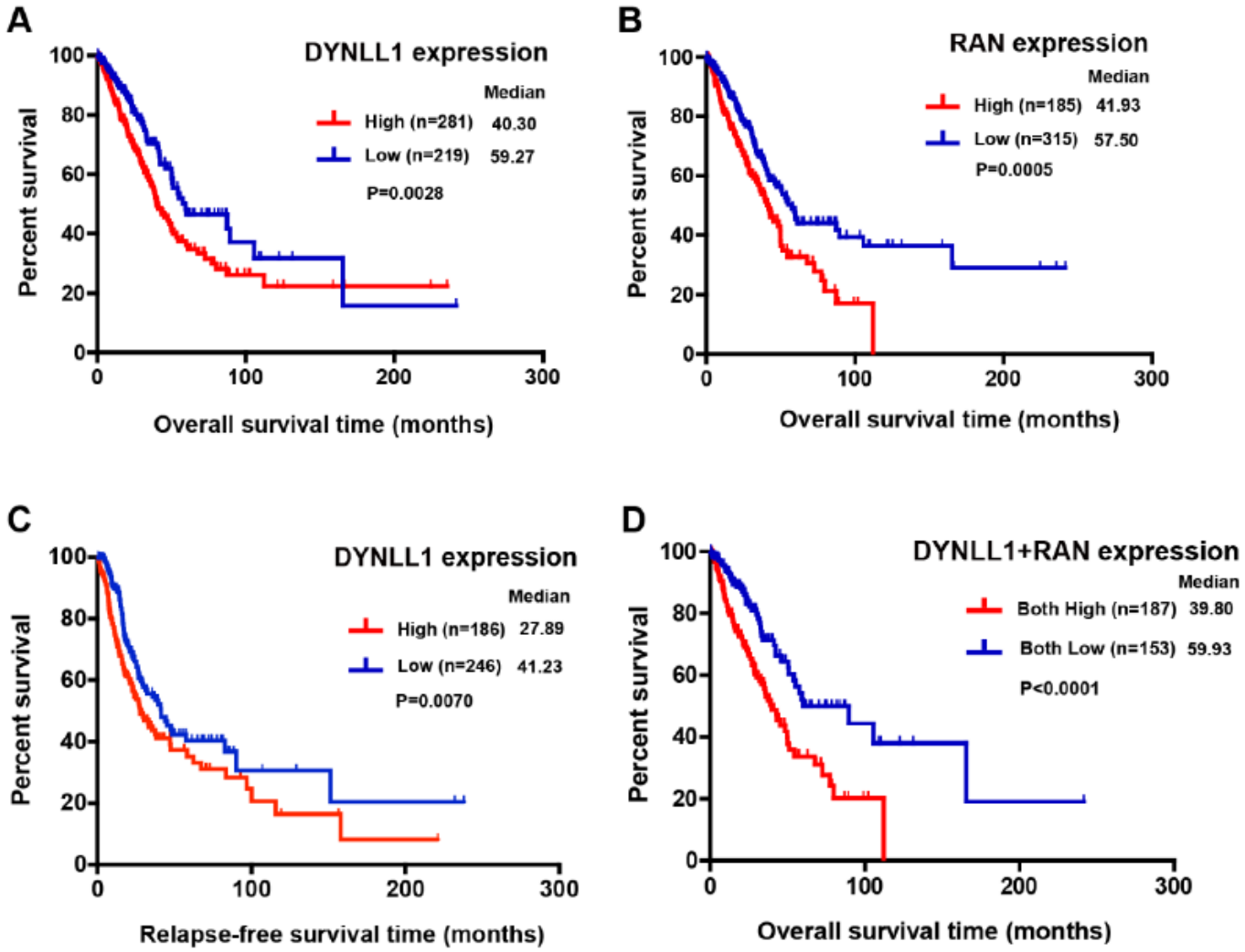

Figure 3

Kaplan-Meier survival curves for assessing the prognostic value of DYNLL1 and RAN. (A) The association between DYNLL1 expression and OS in LUAD. (B) The association between RAN expression and OS in LUAD. (C) The association between DYNLL1 expression and RFS in LUAD. (D) Kaplan–Meier analysis for the OS of LUAD patients according to the expression of DYNLL1 and RAN.

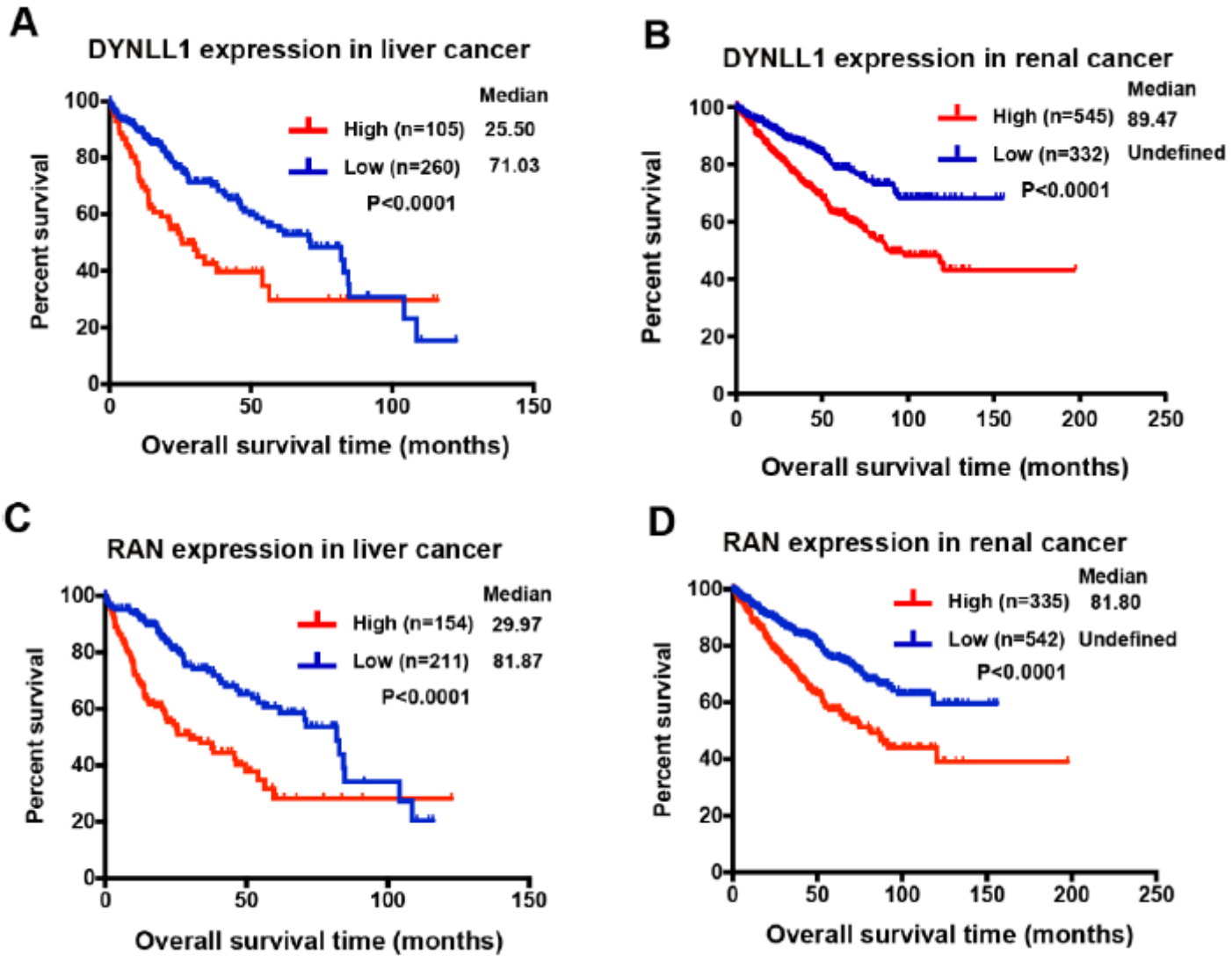

Figure 4

The association between DYNLL1 and RAN expression and survival in Liver and Renal Cancer patients. (A-B) The association between DYNLL1 expression and OS in Liver (A) and Renal (B) Cancer patients. (C-D) The association between RAN expression and OS in Liver (C) and Renal (D) Cancer patients.

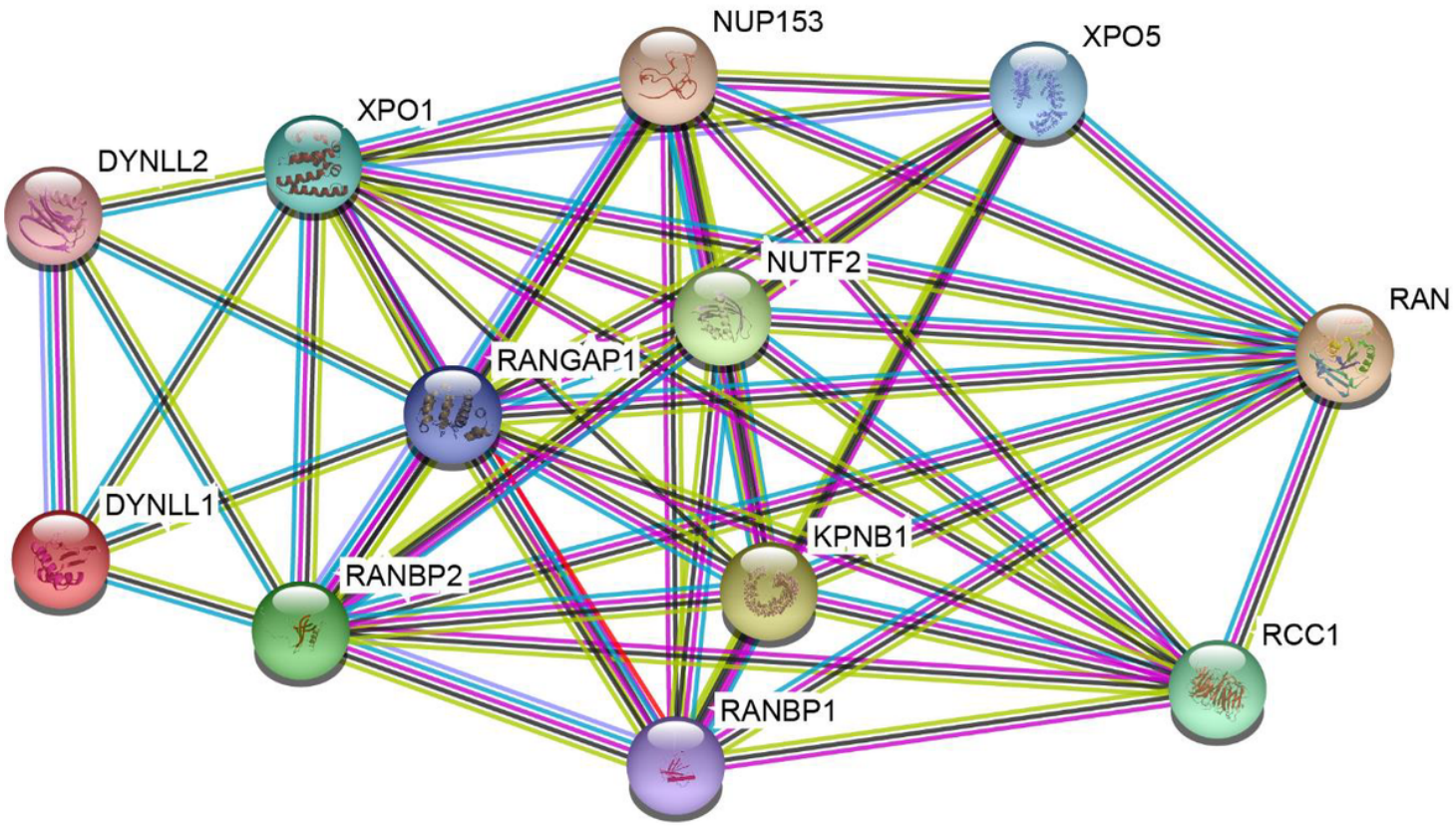

Figure 5

Protein-protein interaction analysis of DYNLL1 and RAN with STRING. Each node represents a different gene. Each line represents a connection between two different genes.

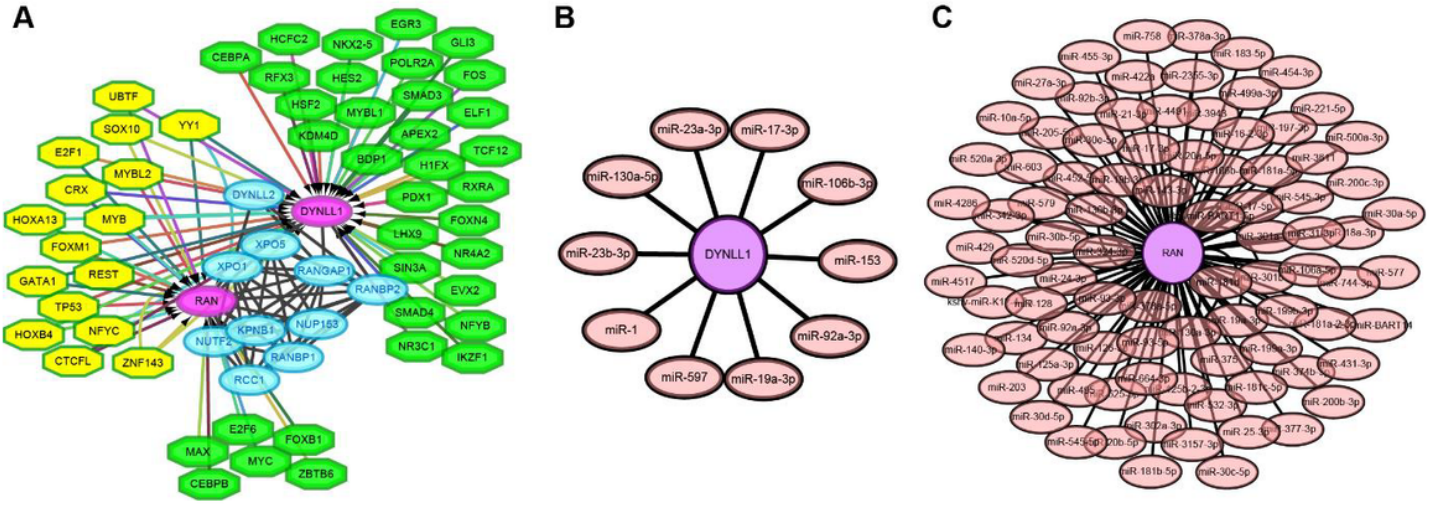

Figure 6

The Target Genes-TF and Target Genes-miRNA Regulatory Network. (A) The network of transcription factors and hub genes. Nodes represent transcription factors indicated with octagon shapes. Yellow indicated that the TFs regulating both DYNLL1 and RAN. Green indicated that the TFs regulating DYNLL1

or RAN alone. (B) The network of DYNLL1 and its related miRNAs. (C) The network of RAN and its related miRNAs.

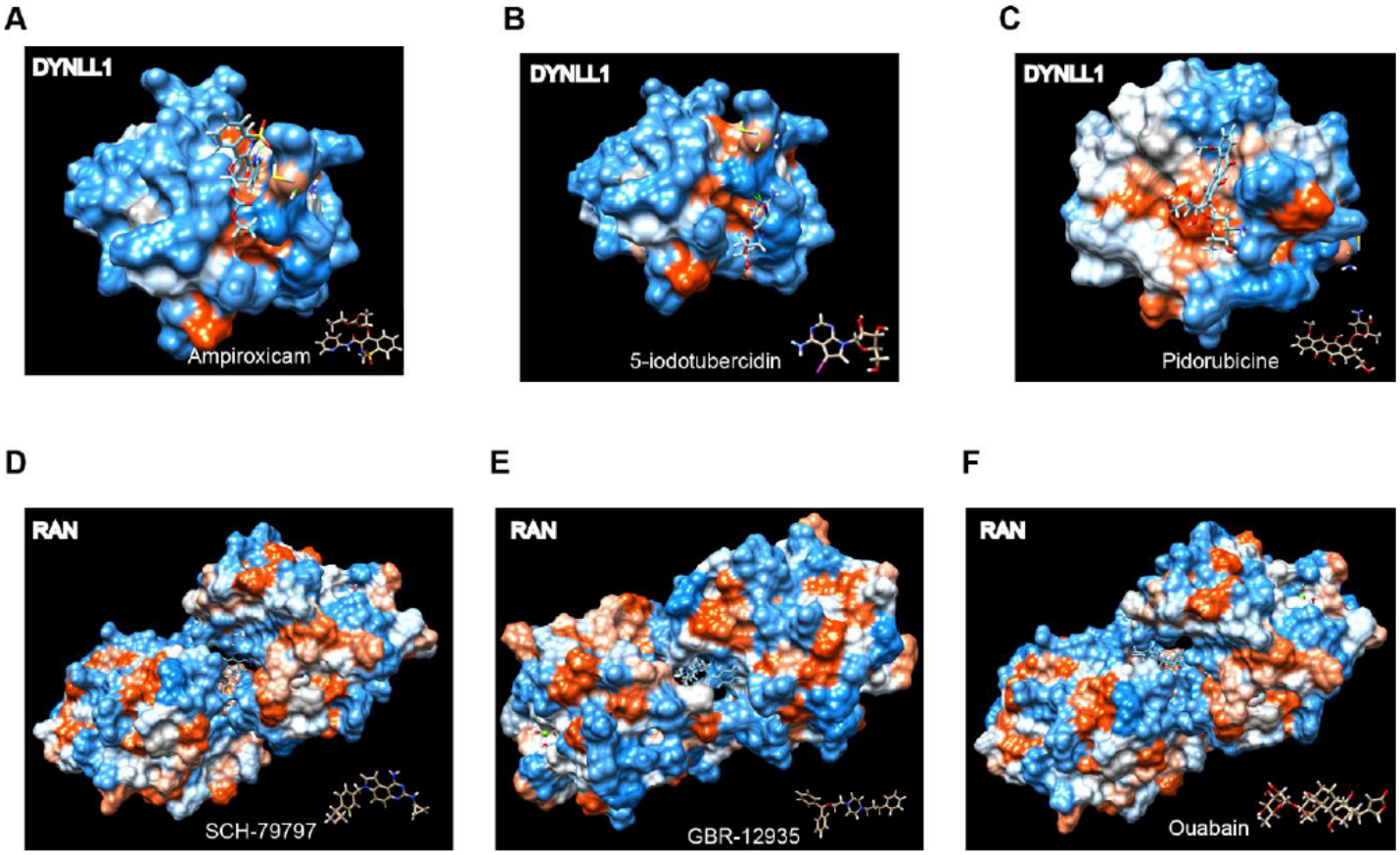

Figure 7

Molecular docking simulation for compounds with DYNLL1 and RAN. (A-C) Molecular docking simulation for DYNLL1 with ampiroxicam (A), 5-iodotubercidin (B), and pidorubicine (C). (D-F) Molecular docking simulation for RAN with SCH-79797 (D), GBR-12935 (E), and ouabain (F).

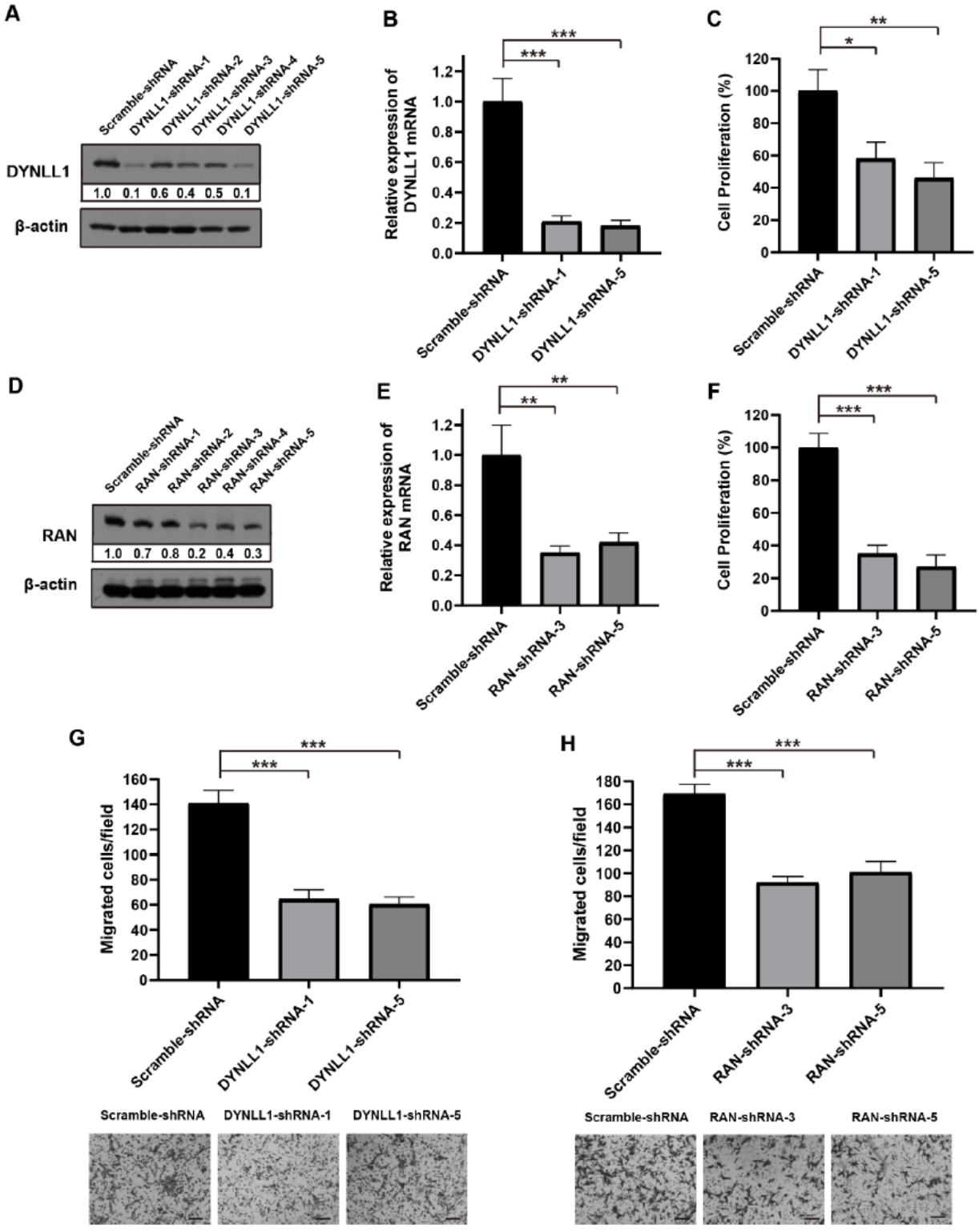

Figure 8

Knockdown of DYNLL1 and RAN inhibit the proliferation and migration of A549 tumor cells. (A) The knockdown efficiency of DYNLL1 was evaluated by Western blot. (B) The knockdown efficiency of DYNLL1 was evaluated by qRT-PCR. (C) The effect of DYNLL1-knockdown on the proliferation of A549 tumor cells. (D) The knockdown efficiency of RAN was evaluated by Western blot. (E) The knockdown efficiency of RAN was evaluated by qRT-PCR. (F) The effect of RAN-knockdown on the proliferation of

A549 tumor cells. (G-H) The control and knockdown A549 tumor cells were seeded in the upper chambers; the lower chambers were supplied with 10% FBS and migrated cell numbers were quantified (n=5 fields/group). Scale bars=100 μm *, P < 0.05, **, P < 0.01, ***, P<0.001.